

## Modelo 3D de geomecánica para caracterización de inestabilidad de fallas y fracturas del campo A y su impacto en las operaciones de optimización de perforación

*Tomás Ricardo Nava Carreón*  
[tomas.ricardo.nava@pemex.com](mailto:tomas.ricardo.nava@pemex.com)  
**Pemex E&P**

*Francis Elisabeth*  
[felisabeth@slb.com](mailto:felisabeth@slb.com)  
**Schlumberger**

*Rafael Zepeda Garduño*  
[rafael.zepeda@pemex.com](mailto:rafael.zepeda@pemex.com)  
**Pemex E&P**

*Vladimir E. Merchan Jaimes*  
[vladimirmerchan@yahoo.es](mailto:vladimirmerchan@yahoo.es)  
**Schlumberger**

*Ismael Díaz Hernández*  
[ismael.diaz@pemex.com](mailto:ismael.diaz@pemex.com)  
**Pemex E&P**

Información del artículo: recibido: mayo de 2015-aceptado: julio de 2015

### Resumen

El campo A se encuentra costa afuera de la bahía de Campeche. La estructura es un bloque anticlinal alóctono, cerrado en su flanco norte por fallas de cabalgamiento. En este campo se ha observado mucha inestabilidad de pozo alrededor de las fallas, generando grandes derrumbes tipo blocosos que han causado severos atrapamientos y sidetrack en el Terciario. Con el fin de optimizar la perforación y mitigar los riesgos, se construyó un modelo geomecánico del subsuelo numérico 3D. Inicialmente, un modelo de geomecánica unidimensional (1D) fue construido utilizando información disponible tal como registros geofísicos, pruebas mecánicas en laboratorio de núcleos, derrumbes y fracturas inducidas interpretados en registros de imagen de pozo, prueba de goteos y eventos de perforación. Un equipo multidisciplinario, incluyendo expertos en física de roca, geo-modelador, geomecánicos, geofísicos, petrofísicos, ingeniero de diseño, y geólogos, combinando sus conocimientos para crear un modelo geomecánico del subsuelo 3D analítico; para asegurar la calidad y reducir la incertidumbre en la construcción del modelo geomecánico del subsuelo, técnicas de inversión sísmica y física de roca se aplicaron para extraer propiedades elásticas de los atributos sísmicos. Propiedades mecánicas de elasticidad estática y de resistencia de la roca, localmente calibrados con ensayos mecánicos en laboratorio fueron espacialmente mejorado usando las velocidades, porosidades y volúmenes resultado de la inversión sísmica y física de la roca. Un cubo de presión de poro para el Terciario fue construido analizando preliminarmente la variación de la velocidad contra el esfuerzo efectivo vertical para identificar el mecanismo generador de presión y calibrado con eventos de perforación de los pozos (influjos y densidad del fluido de perforación). Un cubo de presión de poro en los carbonatos fracturados del Mesozoico fue determinado usando las mediciones directas de presión en el yacimiento. El modelo geomecánico 3D analítico del subsuelo, además de las fallas y fracturas interpretadas, se usaron como entrada para la simulación numérica 3D con métodos de elementos finitos. La compilación de los diferentes derrumbes tabulares y blocosos disponibles, evidencia de inestabilidad de las fallas, ayudaron a calibrar los valores de sus propiedades, (rigidez y resistencia), necesarios para la simulación numérica de inestabilidad de fallas/fracturas y para obtener un

modelo predictivo. Igualmente, la rigidez normal y de cizalla elástica/plástica actuando en las fracturas, fueron utilizados como atributo de geomecánica para calibrar la tasa actual de las pérdidas del fluido de perforación en los carbonatos naturalmente fracturados y predecir para años futuros las áreas con mayor riesgo de pérdidas. Este trabajo presenta los resultados de la integración multidisciplinaria y el impacto para la optimización de perforación caracterizando las deformaciones elasto-plástica actuando en las fallas y fracturas con un modelo de geomecánica del subsuelo 3D numérica para mitigar los problemas de empacamiento en fallas y pérdida de circulación en un yacimiento naturalmente fracturado.

**Palabras clave:** Inestabilidad de fallas, derrumbes blocosos y tabulares, geomecánica, pérdida de circulación, fracturas, optimización de perforación, inversión sísmica, física de roca, modelo de geomecánica 3D y 4D.

## 3D Geomechanics characterization of the faults and fractures of a field and its impact on drilling optimization

### Abstract

The A field is located offshore of the Bay of Campeche. The structure is an allochthonous thrusting anticline with an uplifted block closed in its northern flank by thrusting faults. In this field many wellbore instability have been observed around faults and large blocky cavings caused many stuck pipe and sidetrack in the tertiary formation. In order to optimize drilling and mitigate the risk of crossing faults in the tertiary formation and the severe losses observed in the naturally fractured carbonates, a 3D numerical mechanical earth model was constructed. Initially a 1D Mechanical earth model was built using information in the area such as geophysical logs, mechanical core test, breakouts and induced fractures from image- logs, Leak off test results and drilling events. A multidisciplinary team, including rock physicist, drilling engineer, geo-modeler, geomechanics specialist, geophysicist, petrophysicist, and a geologist, combined their expertise to build a 3D analytical MEM; To ensure the quality and reduce the uncertainty in the mechanical earth model, seismic inversion and rock physics techniques were applied to extract mechanical properties from the seismic attributes. Mechanical properties, locally calibrated from mechanical cores, were spatially improved using velocity, porosity and volumns results from seismic inversion and rock physic analysis. Tertiary pore pressure cube was calibrated against well events and inverted, analyzing the effective stress to velocity transform. Mesozoic pore pressure cube from carbonated formation was inverted using direct measurement in the reservoirs. The 3D analytical mechanical earth model, interpreted faults and fractures was used as an input for the numerical simulation. The various compelling events of tabular and blocky cavings around faults helped calibrate the faults and fractures properties, (rigidity and mechanical parameter), required for numerical simulation of faults and fracture instabilities and obtain a predictive model. The normal and shear plastic strains acting on faults and fractures, were used as Geomechanics attributes to calibrate the exact location of faults instability but also the past and present day rate of mud losses and to predict for future years the location with major risk of fault instability and mud losses in the fractured carbonates reservoir. This paper will present the results of the multidisciplinary integration and the impact for drilling optimization due to fault destabilization, leading to wellbore instability and stuck pipe, in addition on how plastic strain were used as a predicting tool for mud losses and fault instability.

**Keywords:** Fault instability, blocky cavings, fractured carbonates, Geomechanics, mud loss, Drilling Optimization, seismic inversion, rock physics and discrete fracture network.

### Introduction

The A field is located offshore of Mexico in the Bay of Campeche. The A field is mature and is producing from the carbonates of the Cretaceous and Jurassic. There are more than 1000 wells and borehole drilled in this field spread in forty platforms. In some platforms it took more than 3 sidetrack to get to the reservoirs. In the Tertiary formation,

many wells have presented wellbore instability while drilling through faults. The root cause analysis and the record of caving pictures, indicated the main wellbore instability mechanism to be destabilization plane of weakness zones. The other major drilling events are the major losses observed while drilling the naturally fractures carbonates of the Mesozoic formation.

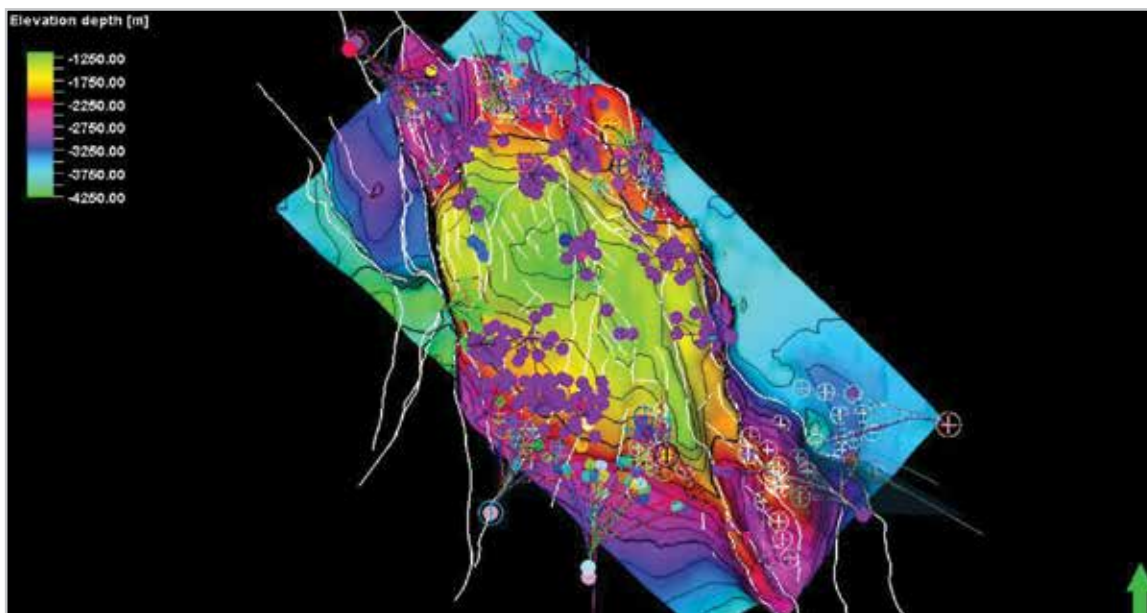


**Figure 1.** Horizontal view of the top upper Cretaceous reservoirs, faults and wells location - Area of ~ 250 km<sup>2</sup>.

With the objective of mitigate wellbore instability problems while crossing faults and major mud losses observed while drilling through the fractured carbonates of the Mesozoic, a full 4D numerical Mechanical Earth Model was constructed.

### Methodology

A one dimensional mechanical earth model (1D M.E.M) was built from available information of the 1000 wells drilled in the A field. Key information such as rock mechanics parameter from laboratory results, breakouts interpreted from image logs and/or oriented caliper and closure pressure interpretation from leak off test information, were key to constrain the characterization of strength, geo-pressures and stresses profiles in the A field. In parallel geophysicist integrated the existing seismic information (CRP gathers from time converted PSDM with normal move out and mute with time migration velocity) and performed seismic inversion to obtain density and velocity (shear and compressional). The seismic inversion results in combination with petrophysical evaluation and rock physics techniques allow to compute a full 3D LithoCube, that capture the lateral variation in the whole field. On the other hands, geologist worked in the structural model by including faults, fractures and horizons to ensure a proper spatial mapping of the reservoirs. Finally, the 1D MEM findings in combinations with the G&G results were integrated in a single platform for 3D and 4D Geomechanics simulations, to predict present and future fault instability

and risk/volume of losses in the discrete fracture network of the Mesozoic formation.

## Building the Mechanical Earth Model

### Geomechanics Data Audit

At the beginning of the study, the A field had already more than 1000 wells and boreholes drilled. A data audit was performed and only information from 898 wells could be retrieved. With this amount of information, the data audit was crucial in order to select and organized the key information, such as geological, formation evaluation, drilling, seismic and production data, required for building the 1D and then the 4D MEM. The following picture describes the quantity of available information gathered during the data audit from the 890 wells and boreholes of the A field. From experience in running similar projects that guaranty a predictive mechanical earth model, a minimum of 40% of available information should be gathered from the extensive “wish” list of necessary information. For the A field the formation evaluation data is falling below the 40% threshold. The data was organized in a comprehensive manner to qualify and quantify the possible impact on the quality of the M.E.M. Most of the MEM steps are also falling below the 40% threshold, **Figures 2 and 3**. However, the spatial characterization from seismic inversion and rock physics techniques will help overcome and mitigate the impact for the mechanical earth modeling.

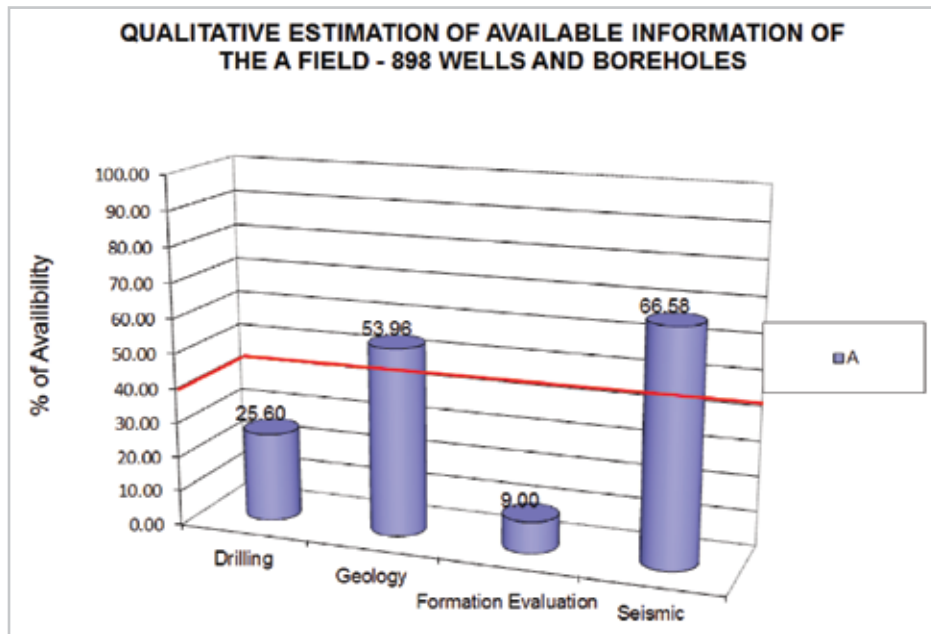


Figure 2. Qualitative estimation of available information in the A field from 898 wells and boreholes.

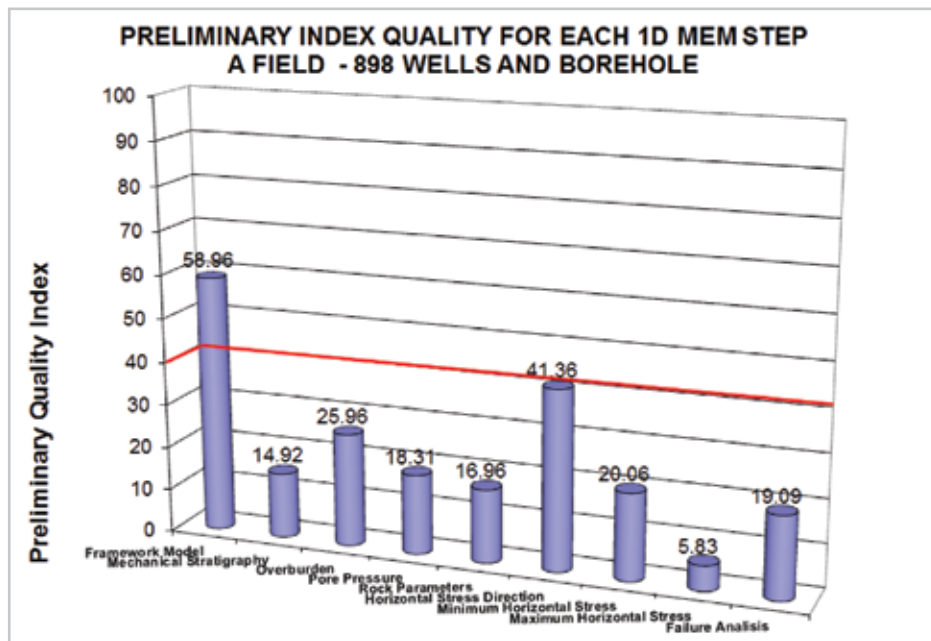


Figure 3. Quantitative estimation of the impact on each 1D MEM steps from available information in the A field from 898 wells and boreholes.

### Root cause analysis of drilling event

A root cause analysis was performed on 47 key wells with enough drilling information and sufficiently spread in the 250 square kilometer area of study. More than 1913

drilling events were analyzed. The most recurring events are partial and total losses in the fractured carbonates of the reservoirs (>50% of all the events). Wellbore instability is second with many issues of cavings tight hole, stuck pipe and drag.

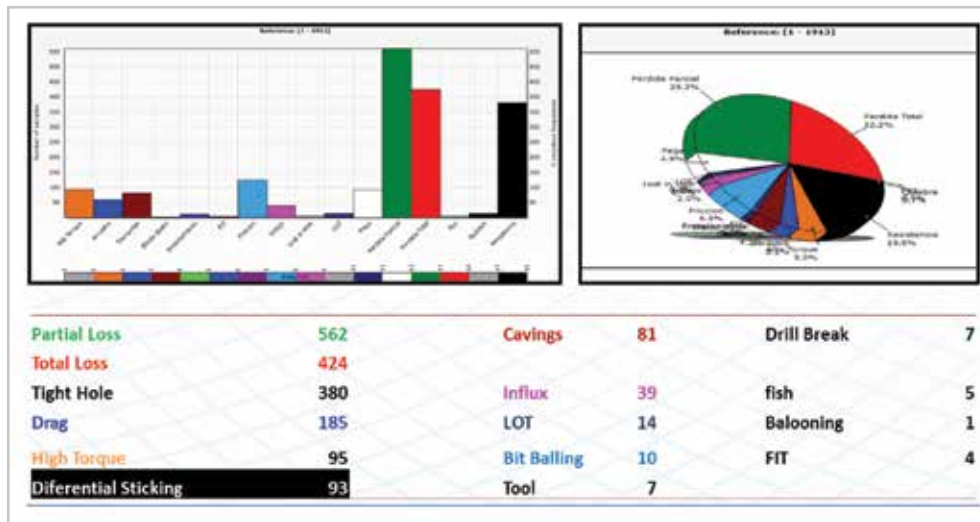


Figure 4. Drilling events statistics from 47 wells of the A field.

With the extension of the A field and the structural complexity, the specific root cause has to be separate by platform. The following will provide all the root cause analysis for the A field:

- Gas and water influx: Inadequate mud weight in permeable formation. In some cases related to the high presence of gas present in the rock matrix of the fractured carbonates.
- Total and partial losses: Mostly due to the presence of open natural fractures in the carbonates of the Mesozoic.
- Wellbore instability (Tight Hole, cavings, high torque, drag, side track): Mainly due to poor hole cleaning,

borehole geometry, high collapse formation, plane of weakness in faults zones.

**Framework model**

The framework model is fundamental when the overall objective of a study is to build a 3D/4D Mechanical Earth Model. For this part of the project, rock physicist, geo-modeler, geophysicist, petrophysicist, and geologist combined their expertise to bring in a single platform all the geological and geophysical results. The seismic inversion analysis allowed capturing the lateral variation of the velocity, (compressional and shear) and density in the field, **Figure 3**.

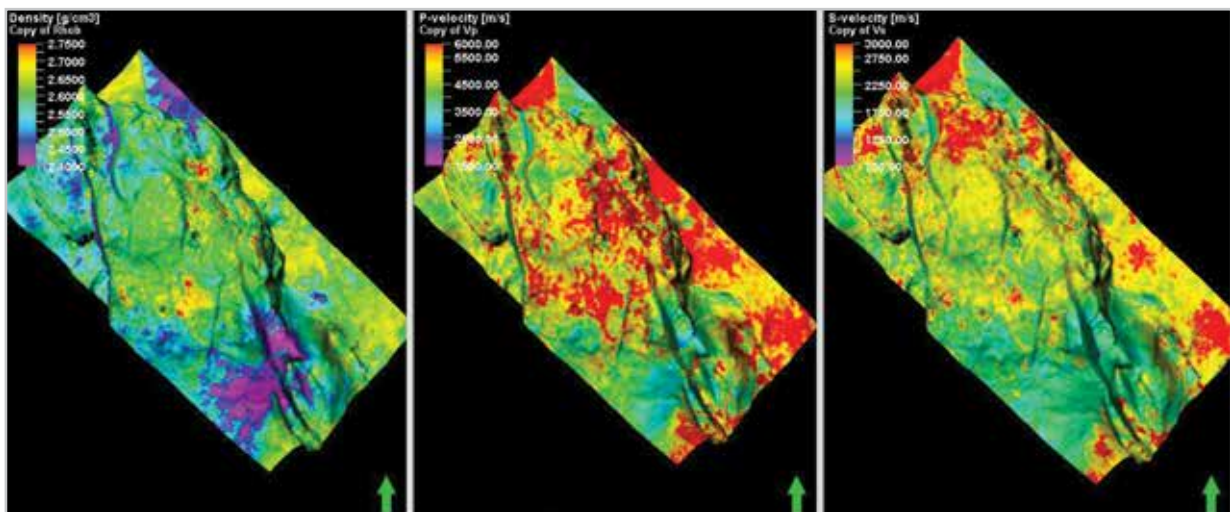
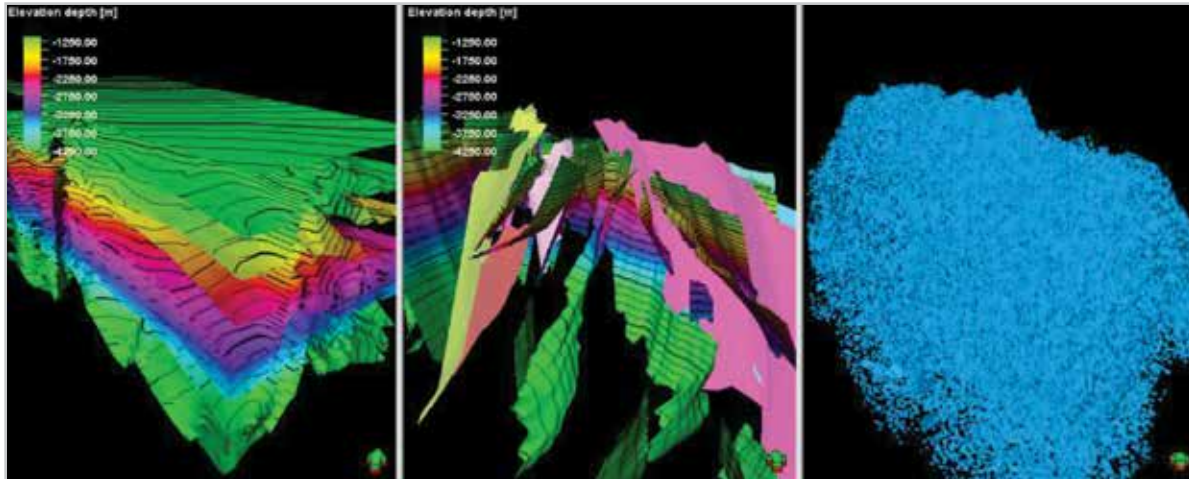


Figure 3. Seismic Inversion results: RHOB, Vp and Vs in the A field, (Upper Cretaceous).

A total of twenty seven (27) horizons and one hundred and sixteen (116) faults were interpreted from tertiary and Mesozoic formations. Finally, the rock physics results in

combination with the natural fractures interpretation from borehole image and seismic discontinuity attributes were integrated to build a discrete fracture network, **Figure 4**.



**Figure 4.** Horizons, faults and fractures network in the A field.

### Mechanical stratigraphy

Lithologies in the A field are a combination of clastic sediments, (shale and sands) and carbonate (Dolomite and mudstone). A rock physics approach combined with petrophysical evaluation allows obtaining 3D volumes of minerals, porosity, (total and effective) and a LithoCube. A total of nine (9) different families were discriminated, (**Figure 5 – Left picture**). However

for geomechanics calculation the concept of mechanical stratigraphy is necessary. By definition, a mechanical stratigraphy is the discrimination of the different family that is believed to have a similar deformation and/or failure behavior. The mud logging information in combination with caliper information, image logs and petrophysical information allow discriminate up to 14 families of mechanical stratigraphy, (**Figure 5 – right picture**).

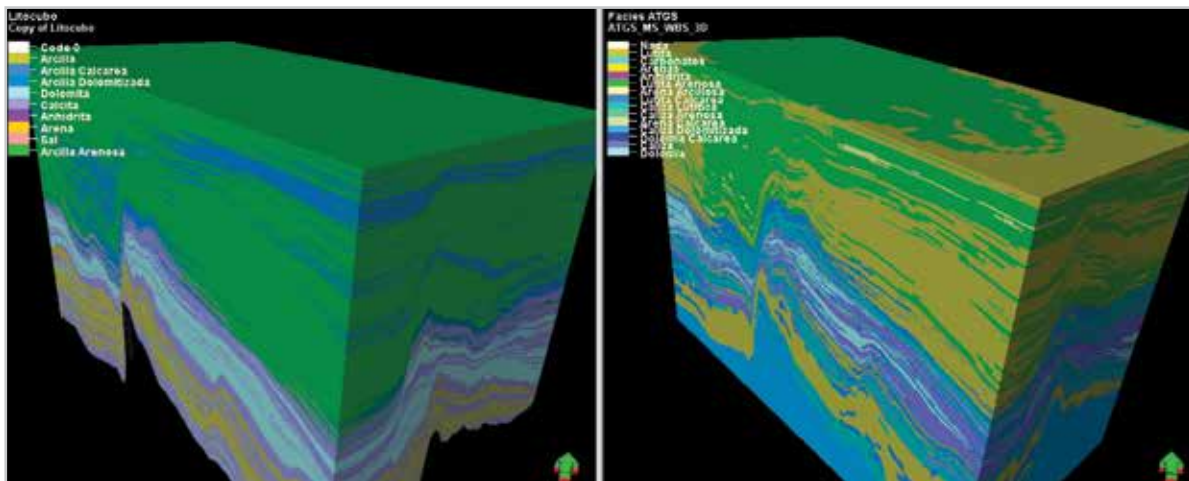


**Figure 5.** Litho Cube vs mechanical stratigraphy cube of the A field.

### Vertical stress and pore pressure

The preliminary vertical stress cube was estimated from the existing density cube and integrated mathematically along the depth. The shallow depth density was also corrected using correlation calibrated from density profile from geotechnical report. The tertiary pore pressure was calibrated against drilling events such as gas and water influx and mud weight profile.

Due to the structural variation in the field, the sonic compressional transit time against true vertical depth is showing a significant spread in values. Trying to fit a unique trend line will over or under predict the pore pressure in some location in the field. It was not possible to find a unique Eaton Trend line and Coefficient that will make the pore pressure prediction match the mud weight profile and gas/water influx.

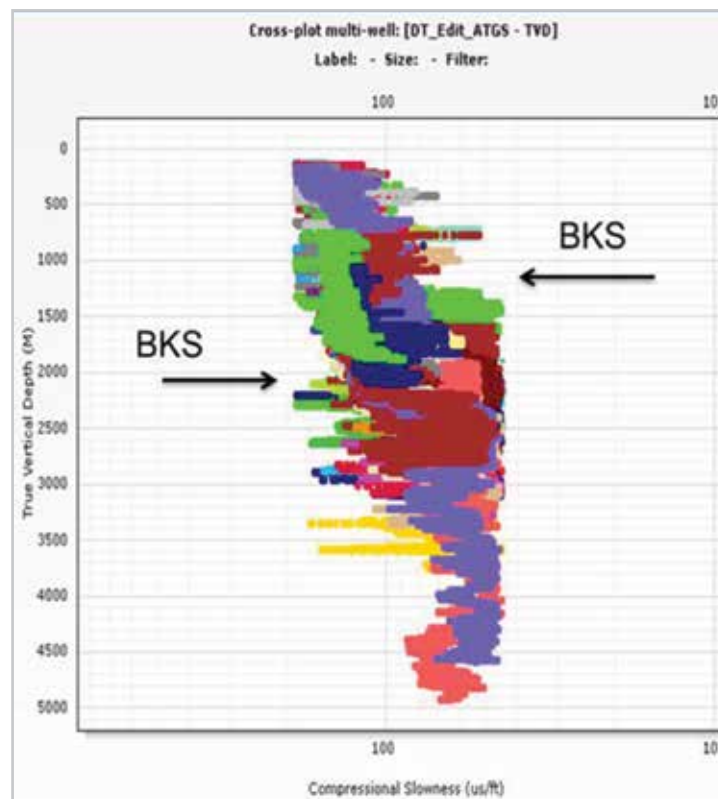


Figure 6. Sonic compressional transit time vs true vertical depth - A field.

An alternative and successful method consisted of plotting the variation of the sonic compressional transit time against the true vertical depth with the zero reference as the true

vertical depth of the top of upper Cretaceous. This method reduced the previous spread of sonic compressional transit time and a unique "trend line" can be fit for the whole field.

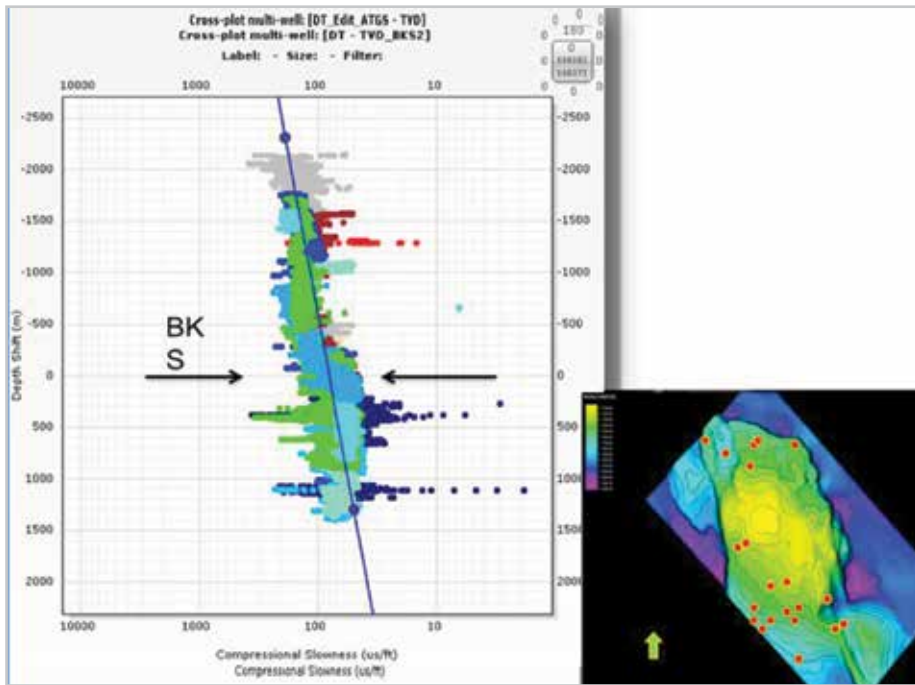


Figure 7. Sonic compressional transit time vs true vertical depth, (Reference - upper Cretaceous) - A field.

This method allows obtain finally a consistent pore pressure prediction in the tertiary for the entire field. The history of measured reservoir pressure was used as an input to calibrate

the pore pressure in the carbonates of the cretaceous and Jurassic reservoirs. **Figures 8 and 9**, presents an example of the final pore pressure profile from 6 wells of the A field.

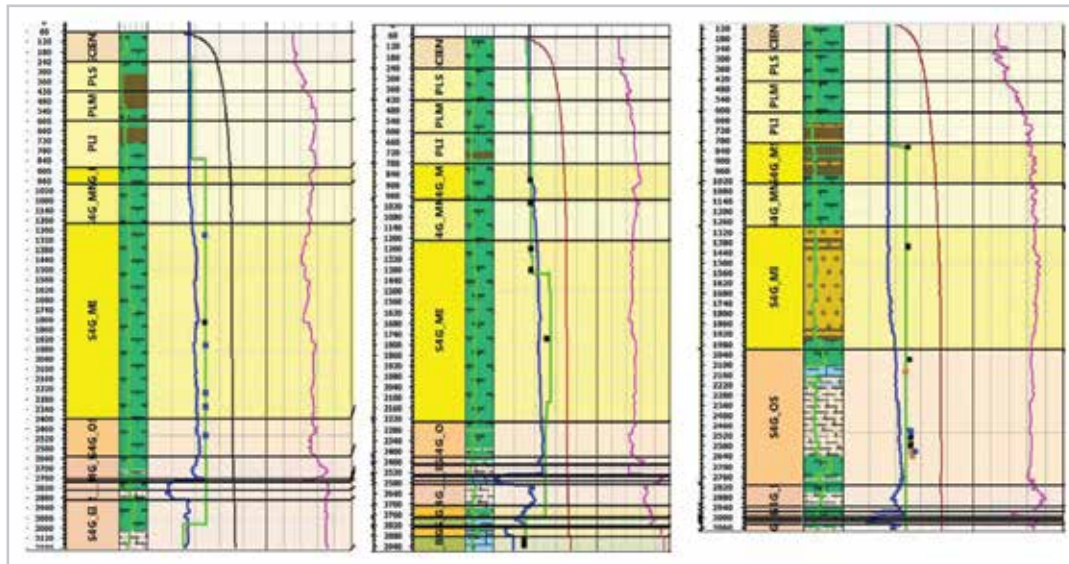


Figure 8. Example 1 of pore Pressure Prediction in 3 offset well in the A field. Pink triangle represents gas and water influx, blue square (Drag), black square (Tight Hole), brown square, (Stuck pipe event).



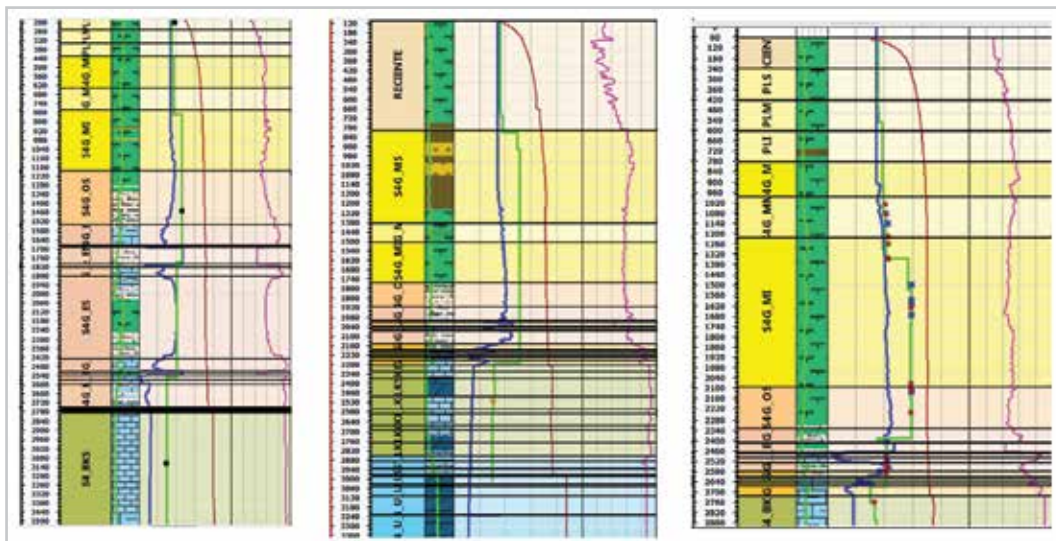


Figure 9. Example 2 of pore pressure prediction in 3 other offset well in the A field. Pink triangle represents gas and water influx, blue square (Drag), black square (Tight Hole), brown square, (Stuck pipe event).

The velocity to effective stress transform calibrated from the wells along with the results of the Vp, Vs, RHOB, mechanical stratigraphy cube and the reservoir pressure

history in the field allow to compute a pore pressure cube for the whole field, Figure 10.

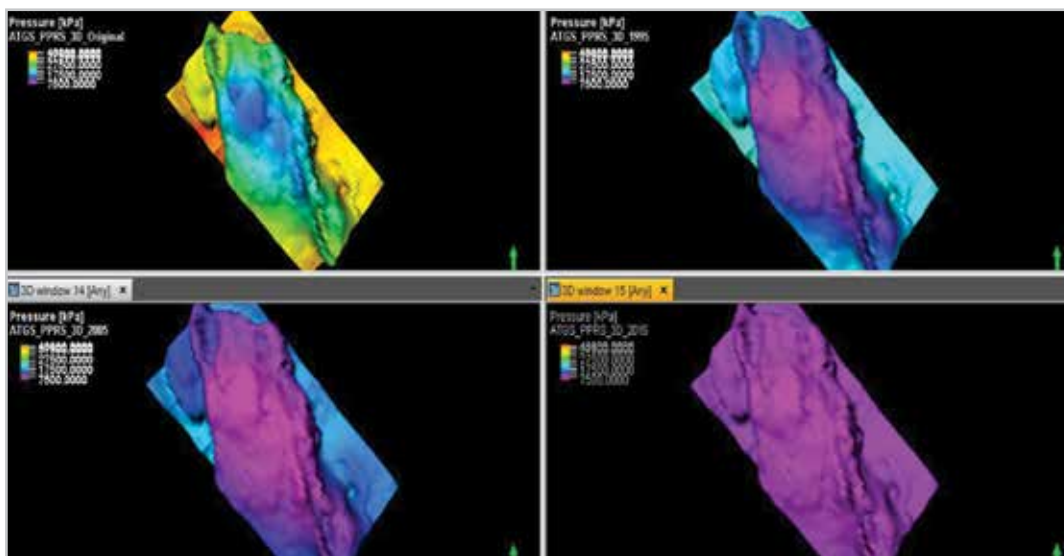
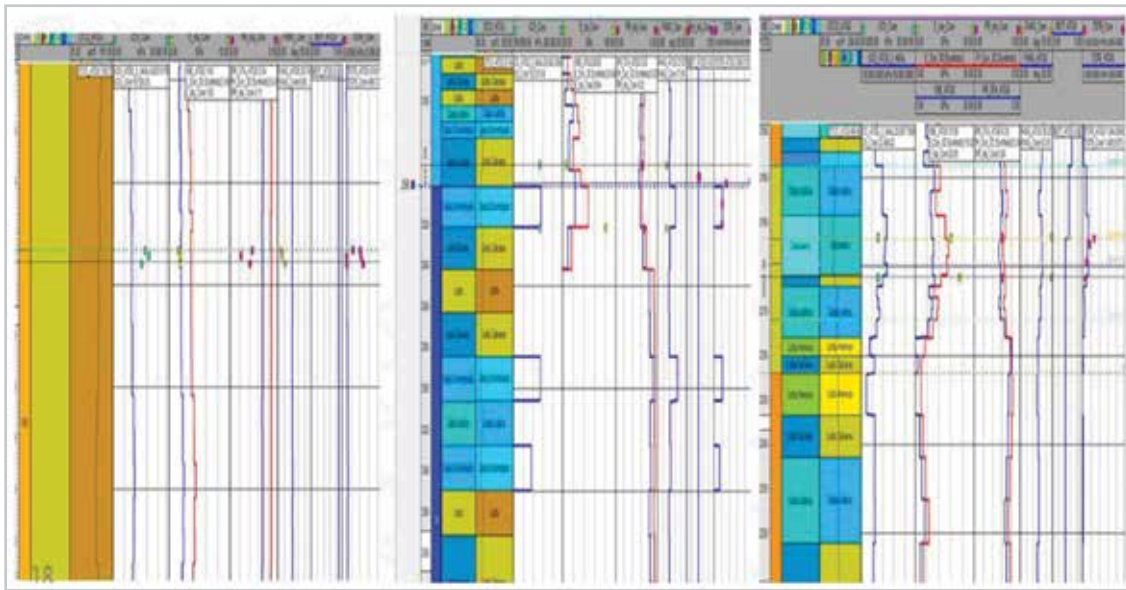


Figure 10. Variation of the reservoir pressure from 1979 to 2015.

### Rock strength parameters

A field has only 3 wells with mechanical core test. Mechanical core test include, hydrostatic, unconfined

compressive, Triaxial and Brazilian test. Local correlations were constructed to match interpreted mechanical parameter values.



**Figure 11.** Validation of mechanical parameter correlation - A field (Tracks: Depth, LithoCube, and Mechanical stratigraphy, UCS, Young Modulus, Poisson's Ratio, Friction Angle and Biot's Coefficient).

These correlations were applied to the seismic inversion, rock physics and mechanical stratigraphy cubes, **Figure 12**.

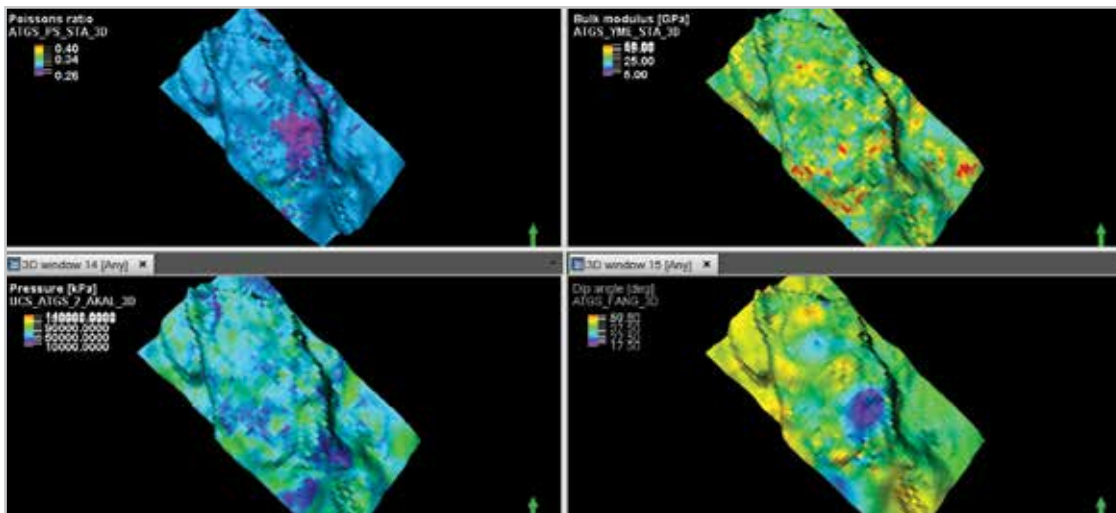


**Figure 12.** 3D Elastic properties (Static Poisson Ratio - Upper Left; Static Young's Modulus-Upper Right) and Rock Strength parameters cubes (Unconfined Compressive Strength - Bottom Right; and Friction Angle - Bottom Right) - Upper Cretaceous.

### Horizontal Stress Direction

Fourteen (14) borehole image logs and one hundred and twenty (120) oriented calipers were interpreted in order to calibrate local stress direction. The general stress direction

seems to be around 120 degrees (horizontal minimum stress), however faults and complex structure is generating many stress rotations. **Figure 13** is showing the complexity of the minimum horizontal stress direction for lower Miocene, Upper Cretaceous and Jurassic Kimmeridgian.

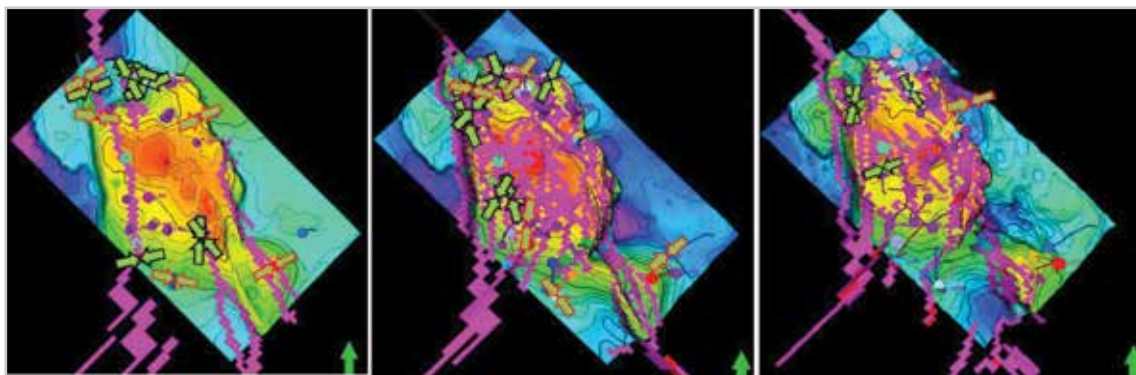


Figure 13. Local stress direction interpreted from image log and oriented caliper. (Left - Lower Miocene; Middle - upper Cretaceous; Right - Jurassic Kim.)

### Analytical fracture gradient and horizontal stresses magnitudes

Leak off test (36), induced mud losses events and upper limit of equivalent circulating density were gathered and analyzed

to obtain fracture gradient and closure pressure calibration points. A Matthews and Kelly<sup>3</sup> type of correlation was established to build the complete 1D fracture gradient profile for the field. The analysis indicated the effective fracture stress to be highly dependent with lithology, **Figure 14**.

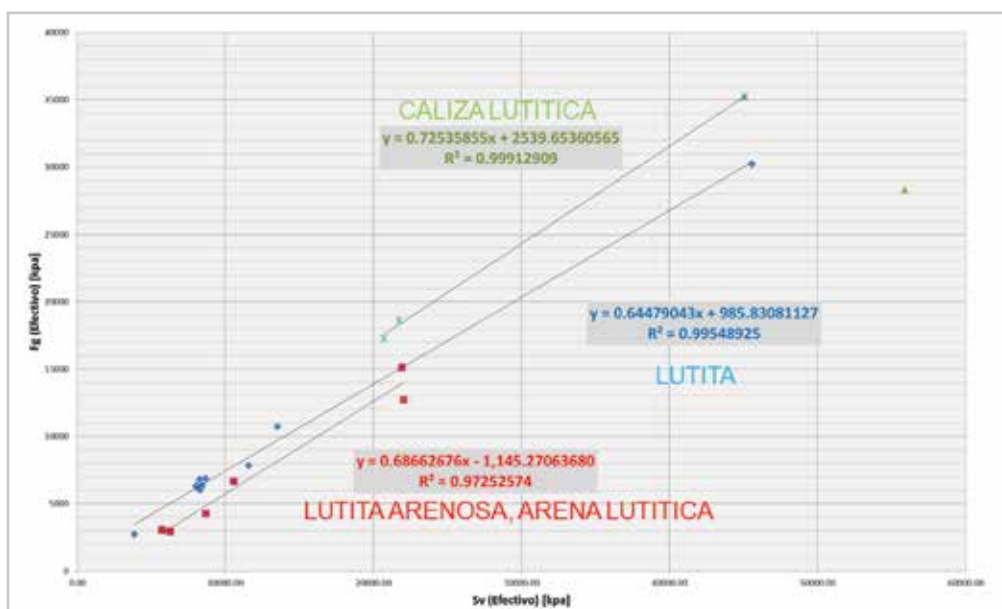


Figure 14. Effective fracture stress vs effective vertical stress for different lithology.

The closure interpretation from the Leak off test indicated an average ratio of six percent (~5%) between fracture gradient and closure pressure. The preliminary stress profile was assumed to be:

$$Sh_{min} = 0.95 * \text{Fracture Gradient}$$

Maximum horizontal stress calibration points were inverted from four different approaches: Adnoy<sup>9</sup> method (Inversion from interpreted breakdown pressure of leak off test or Mini-Frac test). This approach usually overestimates the horizontal stress anisotropy, **Figure 15**. In the following figures we observed maximum horizontal stress anisotropy

up to 30% in tertiary. From experience in this region, the lower bound values of 10% in Tertiary formation are more reasonable values for the horizontal stress anisotropy of this part of the world.

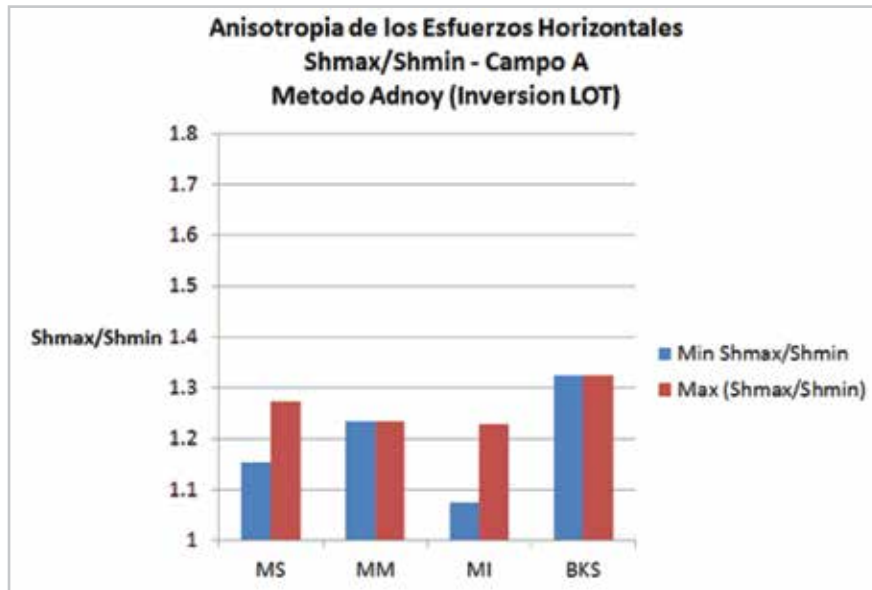


Figure 15. Variation of the minimum and maximum horizontal stress anisotropy along the geological column of the A field - Adnoy method.

A second approach consisted of inverting the horizontal stress anisotropy at the depth where a failure had been interpreted in a borehole image or an oriented caliper, Figure 16. This

method indicated low stress anisotropy in the tertiary (< 10%) and to a maximum of 25% of horizontal stress anisotropy in the carbonates formation of the Jurassic Kim.

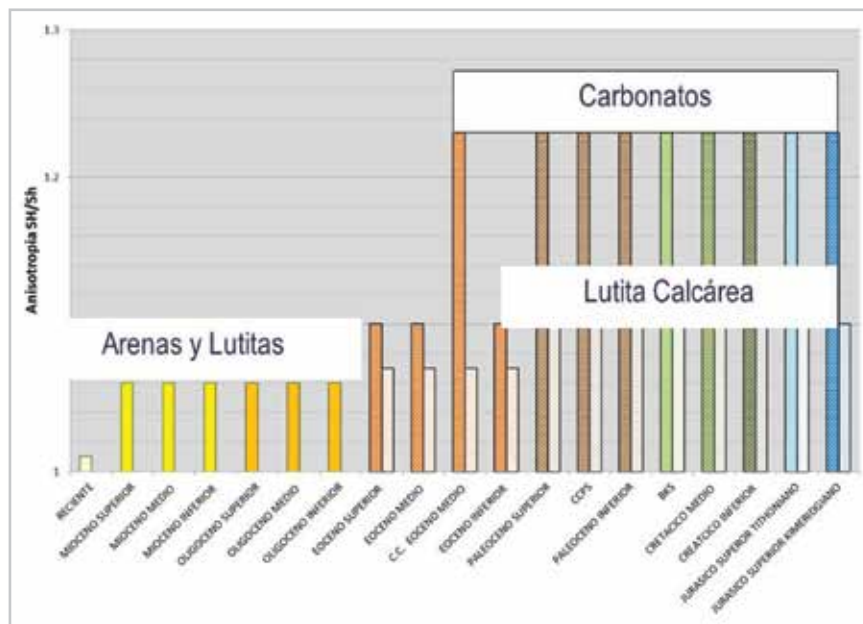
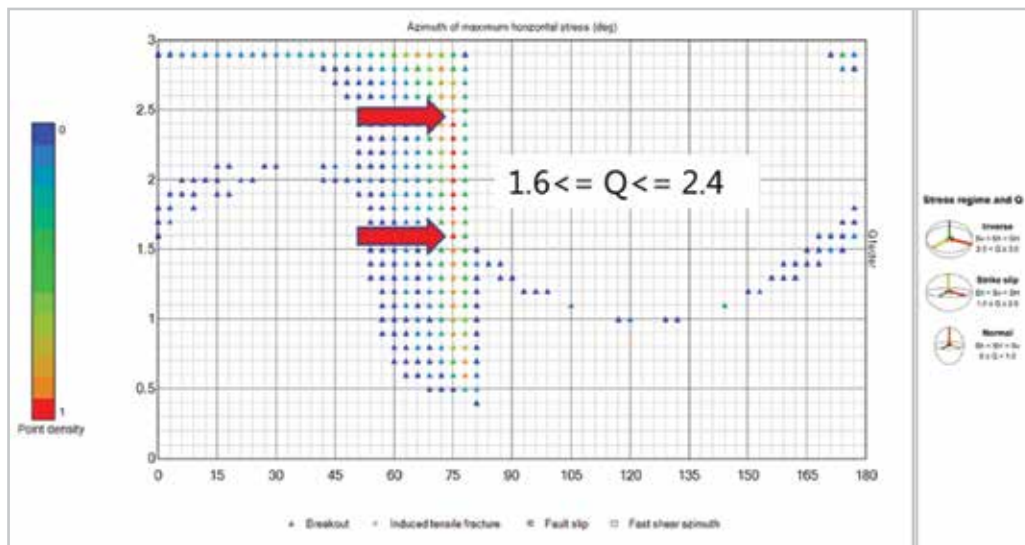


Figure 16. Variation of the horizontal stress anisotropy along the geological column of the A field inverted from failure observed in oriented caliper and borehole image logs.

The method of Etchecopar<sup>4</sup> and al. consist of a least square method from multi-well borehole failure information that investigate all the possible scenario stress direction and shape factor Q, ( $Q = f(R) = (s_2 - s_3) / (s_1 - s_3)$ ) that will match the azimuth of the maximum value of tangential stress

around the borehole (location of the interpreted failure in borehole images and/or oriented caliper), **Figure 17**. Using this technique, the horizontal stress anisotropy in the A field also varies from 10%-20% in Tertiary and up to 40%-70% in the carbonates formation of the Jurassic, **Figure 18**.



**Figure 17.** Example of the possibility of the stress regime and Q factor in Cretaceous in the A field ( $1.6 < Q < 2.4$ ,  $S_{Hmax}$  Azimuth - 75 degrees) - Knowing vertical and minimum stress magnitude,  $S_{Hmax}$  can be easily calculated.

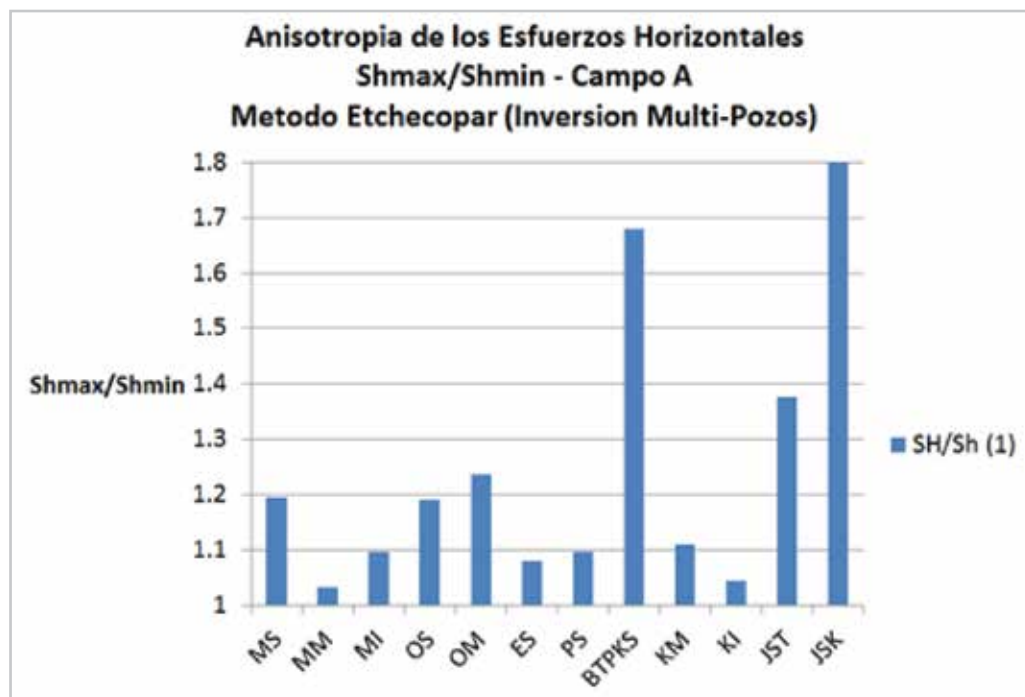


**Figure 18.** Variation of the horizontal stress anisotropy along the geological column of the A field inverted from Etchecopar techniques.

All those calibration points for maximum horizontal stress along with all the interpreted closure pressure for minimum horizontal stress were used to get the horizontal tectonic strain

( $\epsilon_h$ ,  $\epsilon_H$ ) in each formation and for each lithology from the generalized Hooke's law equation – Warspinky<sup>1</sup> to compute a complete horizontal stress profile of the A field, **Figure 19**.

$$d\sigma_h^e = \frac{\nu}{1-\nu} d\sigma_z - \frac{\nu}{1-\nu} \alpha dp + \frac{E}{1-\nu^2} d\epsilon_h + \frac{\nu E}{1-\nu^2} d\epsilon_H$$

$$d\sigma_H^e = \frac{\nu}{1-\nu} d\sigma_z - \frac{\nu}{1-\nu} \alpha dp + \frac{E}{1-\nu^2} d\epsilon_H + \frac{\nu E}{1-\nu^2} d\epsilon_h$$

**Figure 19.** Generalized Hooke's law equation - Warspinky<sup>1</sup>.

Analytical stress regime is normal in the tertiary formation and strike-slip in Mesozoic. An inverse stress regime can be observed locally in some of the carbonates and

shaly carbonated interval of the Eocene, Paleocene and Cretaceous formation, **Figure 20**. The stress regime is consistent with the type of faults observed in the field.

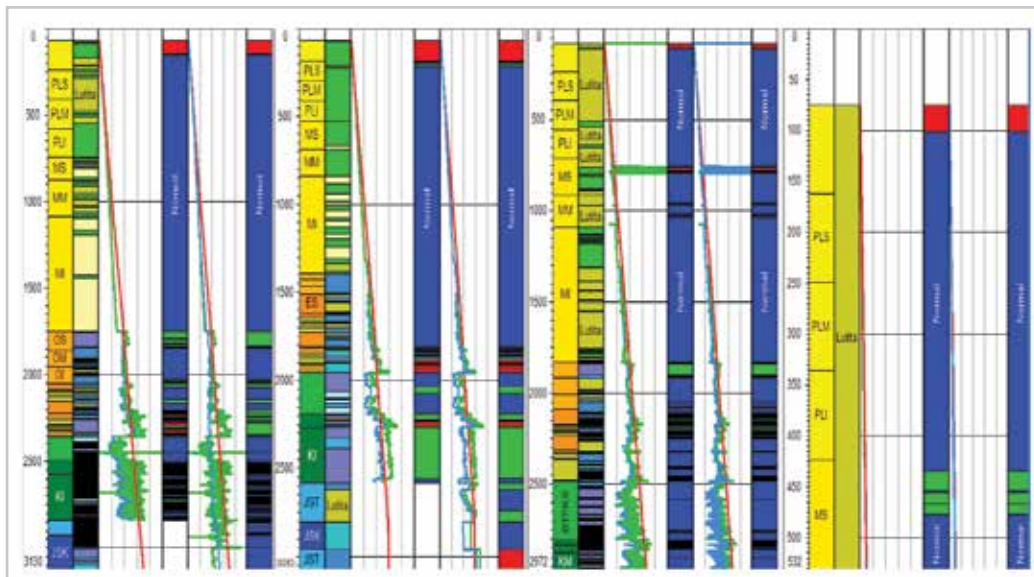


**Figure 20.** Example of the stress regime in four wells of the A field tracks: Depth, geological ages, mechanical stratigraphy, original stresses, original stress regime, actual stresses, and actual stress regime, (Normal regime -blue, Strike-Slip - green; Inverse regime - Red).

### 3D Tertiary Fault Stability Analysis

Much instability has been observed while crossing tertiary faults of the A field, **Figure 21**.

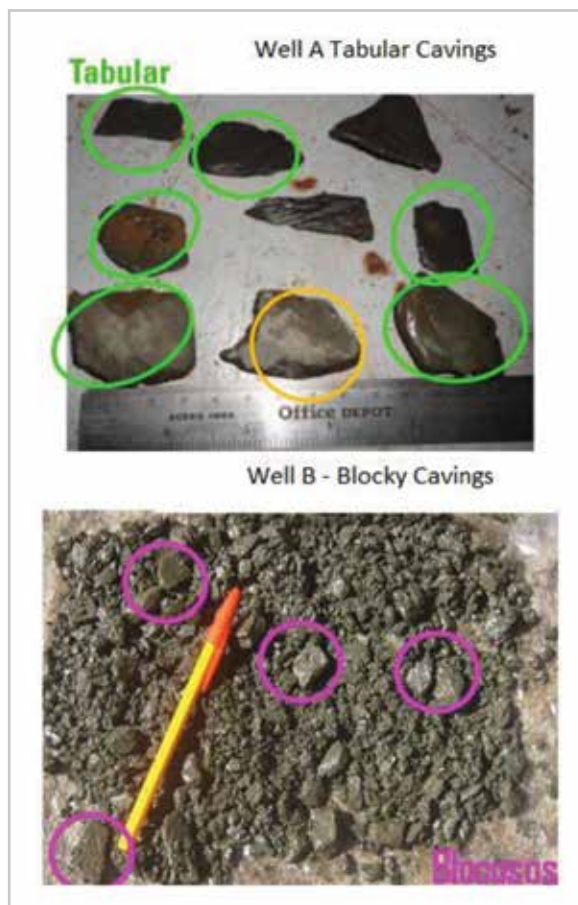


**Figure 21.** Example of tabular and blocky cavings observed in well A and B.

In order to capture better the state of stress acting on faults in the A field, an elastic-plastic numerical simulation approach was conducted to compute the principal stress magnitude and direction. In order to validate the computed numerical stress, they were compared in magnitude and in direction against the 1D analytical horizontal stresses, (**Figures 15** and **16**). A sensitivity analysis on faults mechanical properties was conducted with the objective

of preserving the magnitude and the direction of the principal stresses and to preserve the stability and/or instability observed while drilling.

The numerical model allowed capturing the complexity of the stress in the A field matching locally most of the stress direction interpreted from wells and capturing the rotation observed close to faults and complex geological structure, **Figure 22**.

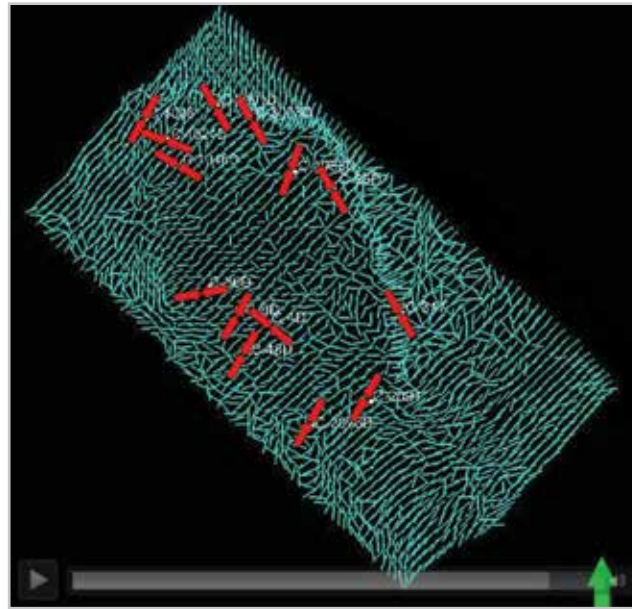


**Figure 22.** Stress direction map (Shmin) vs local stress direction from oriented caliper and borehole image (Cretaceous) - A field.

The numerical achieved a close match with the analytical solution in direction and magnitude, **Figure 23.**

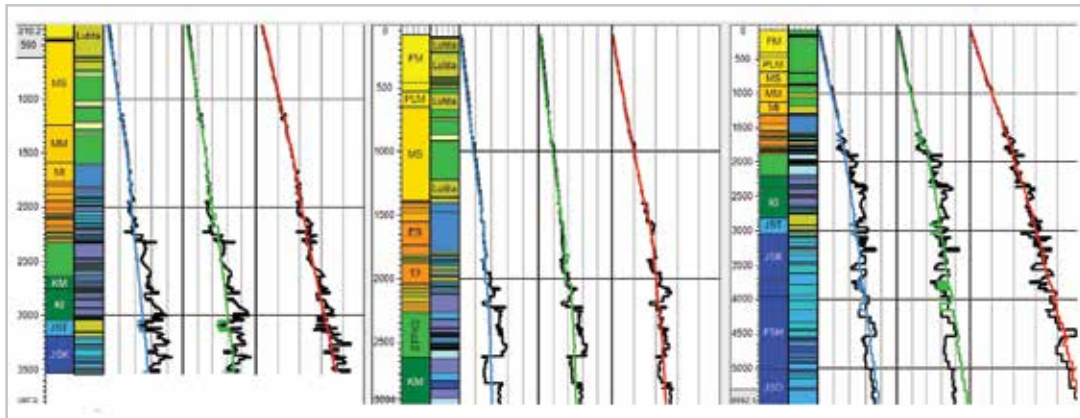


**Figure 23.** Comparison of 3D analytical minimum horizontal stress (Blue curve - Track 1), maximum horizontal Stress (green curve - Track 2), vertical stress (red curve-Track 1), with 3D numerical stresses in black.

The calibration of the numerical stresses was achieved in direction and magnitude and taking in account, faults and fractures mechanical properties. Even though the failure mechanism generating blocky cavings is a “micro” phenomenon, we investigated the possibility of correlating the wellbore stability crossing faults with the magnitude of the strain acting on them where blocky cavings has been observed but also in faults where no blocky cavings were reported. The different strain acting on faults cells analyzed were:

- Elastic normal elastic strain
- Elastic shear strain
- Plastic normal strain
- Plastic shear strain

From those four geomechanics strain acting on faults, the elastic normal strain with values higher than  $0.6E-3$



gave a better prediction of fault stability and instability in comparison with the observed blocky cavings. **Figure 24** is showing a comparison in two wells where blocky cavings

have been reported (Left and middle picture) and one well where no blocky cavings were reported (Right picture) and elastic normal strain are below the  $0.6E-03$  threshold.

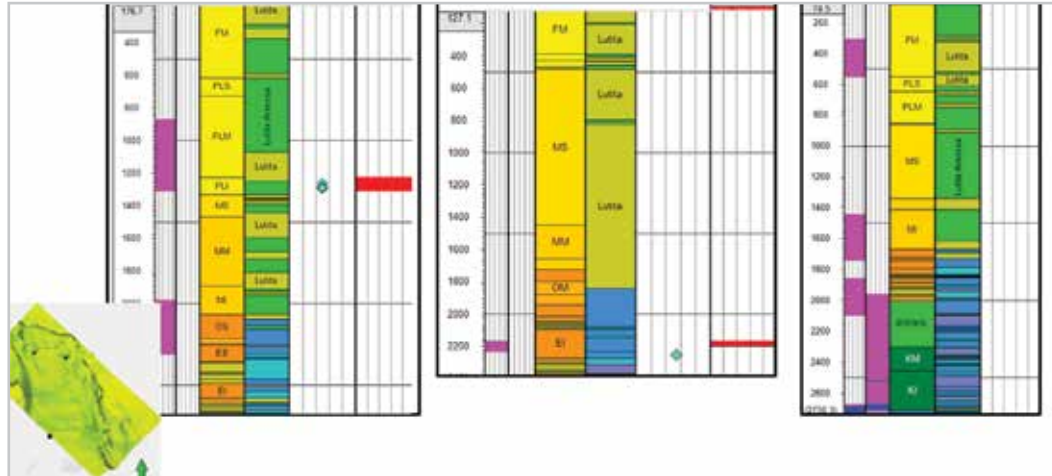


**Figure 24.** Calibration of the faults stability and instability with the elastic normal strain. Tracks: Depth, fault cells, fracture cells, geological column, mechanical stratigraphy, blocky cavings, normal strain acting on fault cells.

**Figure 25** shows, the cells with normal elastic strain value higher than  $0.6E-03$ . We can notice that not all the faults surface present instability. The elastic normal strain can be

used as a criterion to predict fault instability in the tertiary to prepare proper mitigation plan or change trajectory if necessary for future location.

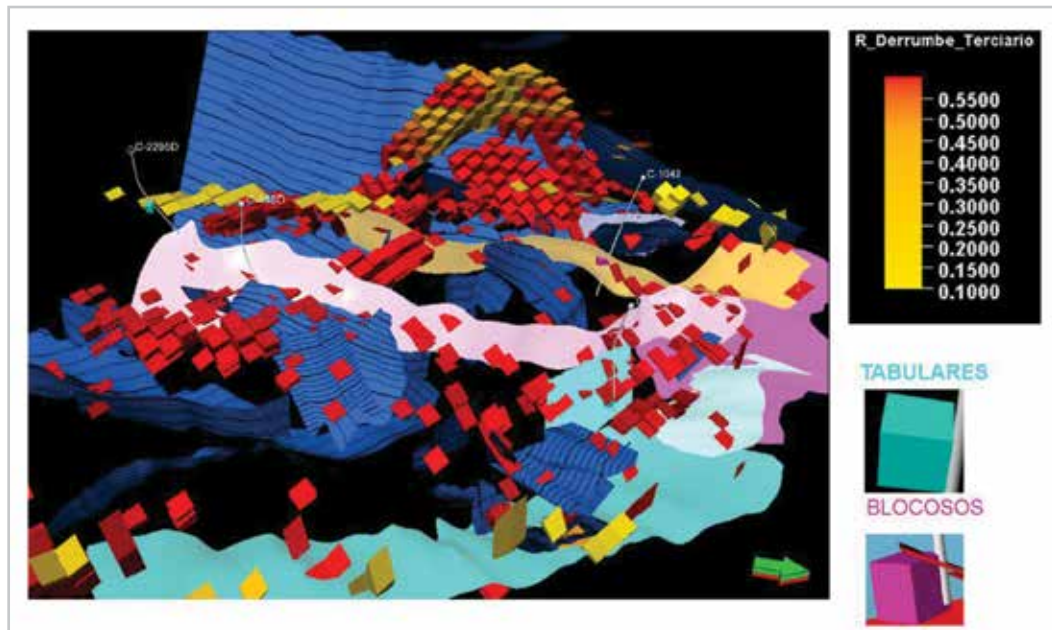


**Figure 25.** 3D visualization of cells with risk of wellbore instability due do fault destabilization.

### Predicting risk and volume of mud losses

With a similar approach than the calibration of the strain with blocky caving, we investigated if we could relate the magnitude of the strain acting on the fractures with the

mud losses events observed in the natural fractures of the Mesozoic formations. From all the strain available in the numerical model, the elastic normal strain gave a better prediction of the volume of losses observed in most of the wells throughout the 30 years of exploitation, **Figure 26**.

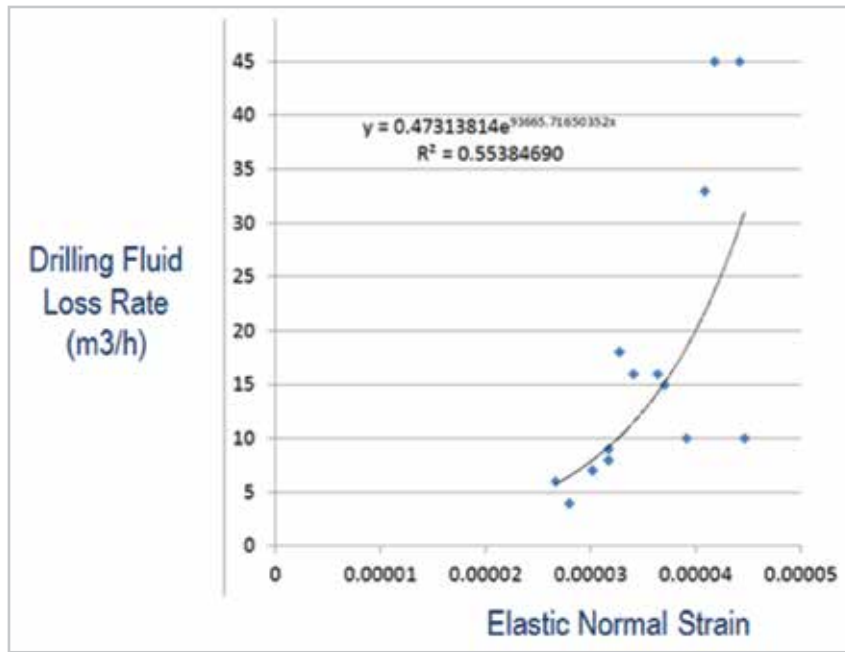


**Figure 26.** Correlation between normal elastic strain and rate of mud losses in key wells from 1979 to 2015.

The calibrated correlation was applied to the cube of elastic normal strain to obtain for present day and future years the expected rate of losses and to visualize areas with higher

and lower risk of total losses. Figure shows the area in upper cretaceous with minor risk of losses less (green cells) and major risk with rate above 40 m<sup>3</sup>/hours (red cells).

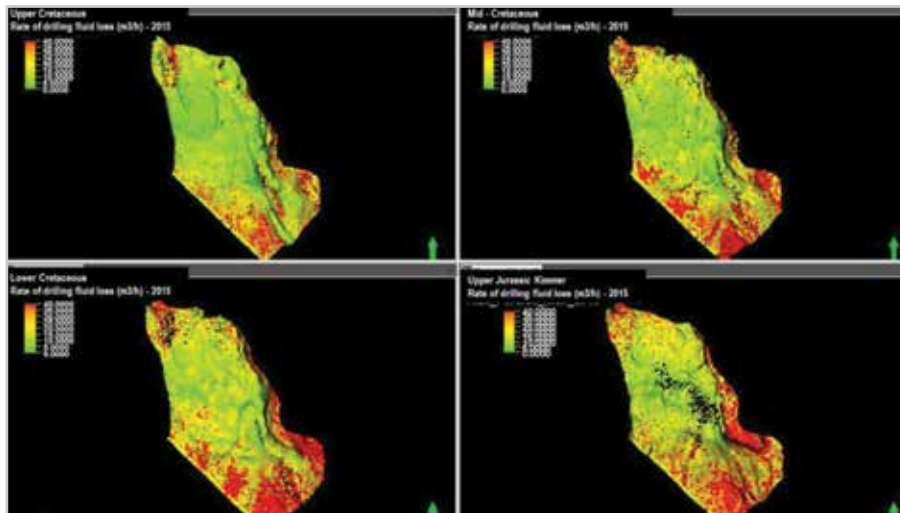


**Figure 27.** Cube of potential rate of losses in 2015 - A field.

## Conclusions

A multidisciplinary study was conducted to characterize the 3D geomechanics behavior of the A field, in order to investigate area of opportunity to mitigate the risk of fault stability in the tertiary and mud losses in the natural fractures of the carbonates of the Mesozoic formation. The study integrated state of the art seismic inversion, rock physics and advanced Geomechanics numerical modeling, in order to reduce uncertainty in the predicted stresses and strains. Even though the finite element is not the right methods to model the “micro” mechanism of rock failure due to plane of weakness, we were able to correlate the elastic and plastic normal/shear strain as a “geomechanics attribute” to predict faults instability in the tertiary and risk/rate of losses in the natural fractures of the Mesozoic formation. With these “geomechanics attribute”, the drilling team are improving the design and planning of wells in the A field, optimize future wellbore trajectory and improve their drilling risk mitigation plans, such as volume and type of lost control material required, and hole cleaning trips.

## Acknowledgments

The authors and co-authors want to thank the management of Pemex in particular Miguel Angel Lozada and Jaime Rios.

The authors and co-authors want also to thank all the participant of the project; Geoscientist, geologist, geophysicist, petrophysicist and drilling engineer that made directly or indirectly the publication of this work possible.

## References

- Aadnoy, B.S., and Hansen, A.K. 2004. Bounds on In-Situ Stress Magnitudes Improve Wellbore Stability Analyses. Presented at the IADC/SPE Drilling Conference, Dallas, Texas, 2-4 March. SPE-87223-MS. <http://dx.doi.org/10.2118/87223-MS>.
- Castillo Castillo, O., and Elizabeth, F.L. 2015. Regional Geomechanics Characterization of the CL Complex (890 Km<sup>2</sup>) for Well Design and DO. 6 International Geomechanics Symposium, Bucaramanga, Colombia, 18-20 March.
- Castillo Castillo, O., Elizabeth, F.L. et al. 2015. Old School vs. New Generation Technique of the Horizontal Maximum Stress Calibration: A Case Studies from EB, A and IK Fields-Mexican Basin-Bay of Campeche. 6 International Geomechanics Symposium, Bucaramanga, Colombia, 18-20 March.
- Desai, C.S., Zaman, M.M., Lightner, J.G. et al. 1984. Thin-Layer Element for Interfaces and Joints. *Int. J. Numer. Anal. Meth. Geomech.* **8** (1): 19–43. <http://dx.doi.org/10.1002/nag.1610080103>.
- Frydman, M., Restrepo, J.D., Palacio, J.E. et al. 2007. Reducing Drilling Risks in Highly Overpressurized Formation: A Case History in Nororient Basin, Argentina. Presented at the Latin American & Caribbean Petroleum Engineering Conference, Buenos Aires, 15-18 April. SPE-108174-MS. <http://dx.doi.org/10.2118/108174-MS>.
- Lee, D., Bratton, T., and Birchwood, R. 2004. Leak-Off Test Interpretation and Modeling with Application to Geomechanics. Presented at the 6th North America Rock Mechanics Symposium, Houston, Texas, 5-9 June. ARMA-04-547.
- Matthews, W.R., and Kelly, J. 1967. How to Predict Formation Pressure and Fracture Gradient. *Oil & Gas Journal* **65** (8): 92-106.
- Palmer, I., Vaziri, H., Willson, S. et al. 2003. Predicting and Managing Sand Production: A New Strategy. Presented at the SPE Annual Technical Conference and Exhibition, Denver, Colorado, 5-8 October. SPE-84499-MS. <http://dx.doi.org/10.2118/84499-MS>.
- Pistre, V., Yan, G.R., Sinha, B. et al. 2009. Determining Stress Regime and Q Factor from Sonic Data. Presented at the SPWLA 50th Annual Logging Symposium, The Woodlands, Texas, 21-24 June. SPWLA-2009-23344.
- Sinha, B.K., Vissapragada, B., Renlie, L. et al. 2006. Horizontal Stress Magnitude Estimation Using the Three Shear Moduli: A Norwegian Sea Case Study. Presented at the SPE Annual Technical Conference and Exhibition, San Antonio, Texas, 24-27 September. SPE-103079-MS. <http://dx.doi.org/10.2118/103079-MS>.
- Sinha, B.K., Wang, J., Kisra, S. et al. 2008. Estimation of Formation Stresses Using Borehole Sonic Data. Presented at the SPWLA 49th Annual Logging Symposium, Austin, Texas, 25-28 May. SPWLA-2008-F.
- Stone, T.W., Xian, C., Fang, Z. et al. 2003. Coupled Geomechanical Simulation of Stress Dependent Reservoirs. Presented at the SPE Reservoir Simulation Symposium, Houston, Texas, 3-5 February. SPE-79697-MS. <http://dx.doi.org/10.2118/79697-MS>.

Téllez, C.P., Elisabeth, F.L., Bentosa, E. et al. 2012. Geomechanics Characterization of the Clastics and Carbonates Formation of Southern Fields of Mexico (2005 - 2009). Presented at the SPE Latin America and Caribbean Petroleum Engineering Conference, Mexico City, Mexico, 16-18 April. SPE-153430-MS. <http://dx.doi.org/10.2118/153430-MS>.

Warpinski, N.R. 1989. Elastic and Viscoelastic Calculations of Stresses in Sedimentary Basins. *SPE Form Eval* 4 (4): 522-530. SPE-15243-PA. <http://dx.doi.org/10.2118/15243-PA>.

## Semblanza de los autores

### Tomás Ricardo Nava Carreón

Ingeniero Petrolero egresado de la Universidad Nacional Autónoma de México.

Ha laborado para el Instituto Mexicano del Petróleo como especialista en terminaciones inteligentes de pozo. Ingresó a Petróleos Mexicanos en las áreas de reingeniería de pozos y nuevas tecnologías, realizando trabajos de control de fluidos no deseados, así mismo en el área de diseño de perforación y terminación de pozos en yacimientos de carbonatos fracturados y arenas deleznable. A la fecha se desempeña como Ingeniero geomecánico con dos años de experiencia en la creación e integración de modelos geomecánicos para perforación y producción.

### Francis Elisabeth

Reconocido y premiado experto de geomecánica principal para Schlumberger e ingeniero con 16 años de experiencia en geomecánica para la optimización de perforación y producción. Su experiencia incluye gerente de operaciones de geomecánica, jefe de equipo y especialista en geomecánica 1D, 3D y 4D.

### Vladimir E. Merchán J.

Ingeniero Civil por la Universidad Industrial de Santander – UIS, Colombia, graduado en el año 2000. Ingresó a la Universidad Nacional de Colombia en el 2001 para cursar estudios de Maestría en Geotecnia. En esta universidad realiza actividades de investigación y consultoría en proyectos de la Facultad de Ingeniería. En el periodo 2005 - 2010 realiza el Doctorado en Ingeniería en la Universidad Politécnica de Cataluña, España. Seguidamente ingresa a la UIS como docente de la Escuela de Ingeniería Civil en cursos de pregrado y postgrado hasta julio de 2012, donde comienza su trayectoria en el sector petrolero como Ingeniero Geomecánico en Schlumberger, hasta la actualidad.

### Ismael Díaz Hernández

Ingeniero Petrolero egresado de la Universidad Nacional Autónoma de México. Cuenta con una especialidad en perforación y mantenimiento de pozos, así como la Maestría en Ingeniería Petrolera y Gas Natural, ambas en la misma institución.

Ingresó a Petróleos Mexicanos en 1999, donde se ha desarrollado en las áreas de mantenimiento a pozos y diseño de la perforación para el Activo de Producción Cantarell.

Actualmente se encuentra laborando en la Subdirección de desarrollo de campos a cargo del plan de perforación para el desarrollo del Campo JSK Sihil.